Synthesis, Characterizations and Chemometric Analysis Approach of Nitrile Functionalized Asymmetrical Dinuclear Silver(I) Di-*N*-Heterocyclic Carbene Complexes

Muhammad Zulhelmi Nazri[a,b*], Mohd Rizal Razali[b] , Sunusi Yahaya Hussaini[c] and Norazah Basar[a,d*]

[a]Innovation Centre in Agritechnology for Advanced Bioprocessing (ICA), Universiti Teknologi Malaysia (Pagoh Campus), Eduhub Tinggi Pagoh 84600 Pagoh, Muar, Johor, Malaysia

[b]School of Chemical Sciences, Universiti Sains Malaysia 11800 Minden, Penang, Malaysia

[c]Department of Chemistry, Kano University of Science and Technology Wudil, Nigeria

[d]Department of Chemistry, Faculty of Science, Universiti Teknologi Malaysia 81310 Skudai, Johor Bahru, Johor, Malaysia

ABSTRACT

A series of novel asymmetrical bis-benzimidazolium salts were synthesized via a two-step alkylation process, yielding the benzimidazolium salts of *N*,*N'*-(ethane/propane/butane-1,2/3/4-diyl)-1-benzylbenzimidazolium-1'-(*n*-benzonitrile)benzimidazolium dibromide (*n* = 2,3,4) (**1Br** – **9Br**). These salts served as carbene precursors for the subsequent formation of nitrile-functionalized asymmetrical silver(I) di-NHC complexes (**Ag1** – **Ag9**) (NHC = N-heterocyclic carbene) through an in-situ deprotonation method using Ag_2O. Comprehensive characterization of the bis-benzimidazolium salts and their corresponding dinuclear silver(I) di-NHC complexes was performed using melting point determination, CHN elemental analyses, FTIR, and ^{1}H- and ^{13}C-NMR spectroscopy. The successful complexation of nitrile-functionalized NHC ligands with silver(I) ions was evidenced by the disappearance of the acidic-carbene proton peak (δ 9.69 – 10.23 ppm) in the ^{1}H-NMR spectra of the complexes. Furthermore, the formation of Ag-C$_{carbene}$ bonds was confirmed by the appearance of characteristic peaks in the ^{13}C-NMR spectra of **Ag1** – **Ag9** (δ 170.89 – 195.90 ppm). To elucidate structure-property relationships, the Principal Component Analysis (PCA) was applied to the NMR spectroscopic data. The Principal Component Analysis (PCA) of the ^{1}H-NMR data revealed distinct clustering of bis-benzimidazolium salts and their respective silver(I) di-NHC complexes, with the first two principal components accounting for 71.40% of the total variance. Similarly, the PCA of the ^{13}C-NMR data explained 72.08% of the total

variance through the first two principal components. These results demonstrate the efficacy of PCA in differentiating and classifying the compounds based on their structural features and functional groups. Moreover, this study highlights the synergistic application of advanced spectroscopic techniques and chemometric analysis in inorganic synthesis chemistry subject and the insights gained from this approach contribute to a deeper understanding of the structural properties and potential applications of these novel NHC complexes, paving the way for future developments in organometallic chemistry and catalysis.

Keywords: *N*-heterocyclic carbene, silver(I) complexes, bis-benzimidazolium salts, nitrile functionalization, principal component analysis

INTRODUCTION

Over the past few decades, the *N*-heterocyclic carbenes (NHCs) containing transition metals have garnered increased interest due to their potential applications in various fields, including catalysis, biological/medical research, nanomaterials, luminescence, and liquid crystal studies [1,2]. Among these, silver(I)-NHC complexes play a crucial role as carbene transfer agents in the creation of other transition and inner transition metal-carbene systems [3]. The stability of NHC compounds is maintained by inductive and mesomeric effects, which make the lone pair of electrons on the carbene carbon more accessible for coordination [4]. This distinct electronic structure offers significant bonding characteristics with transition metals, whose vacant *d*-orbitals are readily available for incoming electrons during complex formation [5].

The design of new functionalized NHCs with nitrogen donor groups has been extensively studied due to their coordination flexibility and ability to enhance coordination stability or substrate activation in metal NHC complexes [6]. These compounds have shown great potential to replace conventional phosphine donors in the synthesis of novel NHC ligands [7]. Various nitrogen donor functionalized NHCs have been well-synthesized, including those with amine, amide, imine, oxazoline, pyrazole, and pyridine functionalities [8]. Moreover, the NHCs often displace ligands such as nitriles, phosphines, THF, CO, THT, pyridines, and DMS [9,10,11]. They can also break dinuclear precursors via aceto or halo bridges to produce monomeric complexes. Depending on the metal and reagent stoichiometry, complexes with three carbene ligands can be synthesized. Compared to phosphines, silver(I)-NHC complexes exhibit greater stability towards air, moisture, and heat due to their strong σ-electron donating properties.

However, research on asymmetric dinuclear silver(I) di-NHC complexes, particularly those derived from imidazole or benzimidazole moieties, remains scarce. Most published studies have focused on symmetrical functionalized silver(I) di-NHC complexes rather than their asymmetric counterparts [12].

This study focuses on the synthesis, preliminary characterizations, and principal component analysis (PCA) of nitrile-functionalized asymmetrical dinuclear silver(I) di-NHC complexes. We chose Ag_2O as the metal source for its ease of coordination with carbon, shorter reaction time, and ability to sustain the reaction under mild conditions compared to alternative silver sources like silver acetate (AgOAc) and silver carbonate (Ag_2CO_3). The application of principal component analysis (PCA) in the study of NHC complex synthesis is a novel approach that can provide valuable insights into the relationships between various synthetic parameters and the resulting complex properties. Meanwhile, the PCA is a powerful statistical technique that can reduce the dimensionality of complex datasets while retaining most of the variation in the data. In the context of NHC complex synthesis, PCA can be used to analyze multiple variables such as reaction conditions (temperature, time, solvent), ligand properties (electronic and steric factors), and complex characteristics (yield, stability, catalytic activity).

A particularly innovative aspect of our research is the application of PCA to ^{1}H- and ^{13}C-NMR spectroscopic data obtained from the synthesized NHC complexes. Since the NMR spectroscopy is a crucial tool for characterizing these complexes, providing detailed information about their structure and bonding. By subjecting the ^{1}H- and ^{13}C-NMR data to PCA, we aim to extract subtle patterns and correlations that may not be immediately apparent from traditional spectral analysis. For ^{1}H-NMR data, the PCA can help identify key proton environments that are most affected by variations in ligand structure or metal coordination. This could reveal important trends in chemical shift changes or coupling patterns that correlate with specific structural features or reactivity patterns of the complexes. In the case of ^{13}C-NMR data, PCA can be particularly valuable for analyzing the carbene carbon signals, which are highly sensitive to the electronic environment of the NHC ligand and its coordination to the metal center. By applying PCA to these spectral data, we may uncover relationships between carbene carbon chemical shifts and factors such as ligand substituents, metal oxidation state, or complex geometry. The combination of PCA with NMR spectroscopy data provides a powerful tool for elucidating structure-property relationships in our nitrile-functionalized asymmetrical dinuclear silver(I) di-NHC complexes. This approach could potentially identify

spectral markers that predict complex stability, reactivity, or catalytic activity, thereby guiding the design of new NHC complexes with tailored properties.

Our research aims to expand the understanding of these novel complexes and their potential applications. By investigating the synthesis, characteristics, and employing PCA in conjunction with NMR spectroscopy data in the study of nitrile-functionalized asymmetrical dinuclear silver(I) di-NHC complexes, we hope to contribute to the growing body of knowledge in this field. This multifaceted approach, combining synthetic chemistry with advanced statistical analysis of spectroscopic data, represents a significant step forward in the rational design and development of new NHC complexes. The insights gained could potentially uncover new avenues for their use in catalysis, medical applications, or materials science, and provide a framework for future studies in the field of organometallic chemistry.

MATERIALS AND METHODS

Materials

Benzimidazole (Merck, 99%), Potassium hydroxide pellets (Merck, 85%), Benzyl chloride (Sigma-Aldrich, 99%), 2-(bromomethyl)benzonitrile (Sigma-Aldrich, 97%), 3-(bromomethyl)benzonitrile (Sigma-Aldrich, 95%), 4-(bromomethyl)benzonitrile (Sigma-Aldrich, 99%), 1,2-dibromoethane (Merck, 99%), 1,3-dibromopropane (Sigma-Aldrich, 99%), 1,4-dibromobutane (Merck, 98%), Silver oxide (Merck, 99%), Potassium hexafluorophosphate (Acros, 99%), Celite 545 (Merck, particle size 0.02 – 0.1 mm), Dimethyl sulfoxide (QrëC), Chloroform (R&M Chemicals), Acetonitrile (QrëC), Diethyl ether (R&M Chemicals), Dichloromethane (QrëC), Methanol (QrëC), Ethanol (QrëC), n-hexane (QrëC), Dimethyl sulfoxide-d_6 with TMS (0.03%) (Merck, 99.8% atom %D). The N-(n-benzonitrile)benzimidazole (where n = 2, 3 and 4) and the N-(2-bromoethyl)-N'-benzylbenzimidazolium bromide, **i·Br** were prepared according to reported literature with minor modification [13]. The yield obtained for all products were 90%.

Instrumentations

The melting points were determined using Stuart Scientific SMP-1. The FTIR spectra of all compounds were recorded using Perkin Elmer Spotlight 200 FT-IR Microscopy System in the

range 4000 – 600 cm^{-1}. The ^{1}H- and ^{13}C-NMR were obtained at room temperature on a Bruker 500 MHz Ascend spectrometer from solution in DMSO-d_6 using TMS as an internal reference. The spectra were recorded in the ranges of 0 – 11 ppm and 0 – 200 ppm for ^{1}H- and ^{13}C-NMR, respectively. The resonance appeared in a singlet (s), doublet (d), triplet (t), quartet (q) and multiplet (m). All instruments are available at the School of Chemical Sciences, Universiti Sains Malaysia (USM).

The synthesis of N-(3-bromopropyl)-N'-benzylbenzimidazolium bromide, ii·Br

In a round bottom flask, benzyl benzimidazole (1.50 g, 7.20 mmol) was reacted with 1,3-dibromopropane (5 mL, 24.76 mmol) in neat. The mixture was refluxed at 80 – 100 °C for 24 h. The brown precipitate appeared as the crude product was washed with dichloromethane (3 × 10 mL). **Yield**: 2.30 g (78 %), **MP**: 202 - 204 °C. **FTIR** (ATR, cm^{-1}): 3127, 3027 (Csp^3-H$_{arom}$ stretching); 2950 (Csp^3-H$_{aliphatic}$ stretching); 1612, 1483, 1446 (C$_{aromatic}$=C$_{aromatic}$ stretching); 1262 (C-N stretching). **^{1}H NMR** (500 MHz, d_6-DMSO) in δ ppm: 3.62 (2H, m, N-CH$_2$C**H**$_2$CH$_2$Br), 3.70 (2H, t, N-C**H**$_2$CH$_2$CH$_2$Br, J = 10 Hz), 4.74 (2H, t, N-CH$_2$CH$_2$C**H**$_2$Br, J = 5 Hz), 5.88 (2H, s, N-C**H**$_2$-Ar), 7.38 – 7.64 (5H, m, arene-**H**), 7.67 – 8.19 (4H, m, benzimi-**H**), 10.29 (1H, s, ArCH$_2$-N-C**H**-N-CH$_2$(CH$_2$)$_2$Br). **^{13}C NMR** (125 MHz, d_6-DMSO) in δ ppm: 31.31 (N-CH$_2$CH$_2$**C**H$_2$Br), 31.94 (N-CH$_2$**C**H$_2$CH$_2$Br), 46.10 (N-**C**H$_2$CH$_2$CH$_2$Br), 50.45 (N-**C**H$_2$-Ar), 114.26, 114.43, 127.14, 128.70, 128.89, 129.14, 129.38, 131.30, 131.80, 134.39 (arene-**C**/benzimi-**C**), 143.22 (ArCH$_2$-N-**C**H-N-CH$_2$(CH$_2$)$_2$Br). Anal. Calc. for C$_{17}$H$_{18}$Br$_2$N$_2$: C, 61.83; H, 5.49; N, 8.48%. Found: C, 60.89; H, 5.56; N, 8.52%

The synthesis of N-(2-bromobutyl)-N'-benzylbenzimidazolium bromide, iii·Br

The preparation of *N*-(2-bromobutyl)-*N'*-benzylbenzimidazolium bromide is similar to that *N*-(2-bromopropyl)-*N'*-benzylbenzimidazolium bromide but using 1,4-dibromobutane (5 mL, 23.16 mmol) instead of 1,3-dibromopropane. **Yield**: 2.20 g (72 %), **MP**: 203 - 205 °C. **FTIR** (ATR, cm^{-1}): 3128, 3033 (Csp^3-H$_{arom}$ stretching); 2969 (Csp^3-H$_{aliphatic}$ stretching); 1607, 1493, 1456 (C$_{aromatic}$=C$_{aromatic}$ stretching); 1266 (C-N stretching). **^{1}H NMR** (500 MHz, d_6-DMSO) in δ ppm: 0.88 (2H, m, N-CH$_2$CH$_2$C**H**$_2$CH$_2$Br), 1.20 – 1.78 (2H, m, N-CH$_2$C**H**$_2$CH$_2$CH$_2$Br), 4.45 (2H, , N-C**H**$_2$CH$_2$CH$_2$CH$_2$Br, J = 5 Hz), 5.20 (2H, s, N-CH$_2$CH$_2$CH$_2$C**H**$_2$Br), 5.77 (2H, s, N-C**H**$_2$-Ar), 7.40 – 7.46 (5H, m, arene-**H**), 7.83 – 8.10 (4H, m, benzimi-**H**), 9.99 (1H, s, ArCH$_2$-

N-C**H**-N-CH$_2$(CH$_2$)$_3$Br). **^{13}C NMR** (125 MHz, d_6-DMSO) in δ ppm: 13.88 (N-CH$_2$CH$_2$CH$_2$**C**H$_2$Br), 19.45 (N-CH$_2$CH$_2$**C**H$_2$CH$_2$Br), 30.92 (N-CH$_2$**C**H$_2$CH$_2$CH$_2$Br), 47.06 (N-**C**H$_2$CH$_2$CH$_2$CH$_2$Br), 50.56 (N-**C**H$_2$-Ar), 113.50, 114.47, 127.38, 129.26, 131.12, 131.41, 131.70, 131.32 (arene-**C**/benzimi-**C**), 143.68 (ArCH$_2$-N-C**H**-N-CH$_2$(CH$_2$)$_3$Br). Anal. Calc. for C$_{18}$H$_{20}$Br$_2$N$_2$: C, 62.80; H, 5.86; N, 8.14%. Found: C, 61.56; H, 5.86; N, 8.01%

General procedure for the synthesis of N,N'-(ethane-1,2-diyl)-1-benzylbenzimidazolium-1'-(n-benzonitrile)benzimidazolium dibromide, (1Br – 3Br) (n = 2, 3 & 4) derivatives

The *N*-(2-(bromomethyl)benzonitrile)benzimidazole (0.59 g, 2.52 mmol) was added to the synthesized *N*-(2-bromoethyl)-*N'*-benzylbenzimidazolium bromide, **i·Br** (1.00 g, 2.52 mmol) dissolved in acetonitrile (20 mL) and the reaction mixture was refluxed for 24 h at 80 – 100 °C. Upon cooling at room temperature, the precipitate was formed then filtered and washed with acetonitrile (5 mL) and diethyl ether (2 × 3 mL).

N,N'-(ethane-1,2-diyl)-1-benzylbenzimidazolium-1'-(2-benzonitrile)benzimidazolium dibromide, 1Br

White solid (powder). **Yield**: 1.22 g (75 %), **MP**: 241 - 243 °C. **FTIR** (ATR, cm^{-1}): 3027 (Csp^3-H$_{arom}$ stretching); 2966 (Csp^3-H$_{aliphatic}$ stretching); 2234 (C≡N stretching); 1449 (C-N stretching). **^{1}H NMR** (500 MHz, d_6-DMSO) in δ ppm: 5.28 (4H, s, N-C**H**$_2$C**H**$_2$-N), 5.78 (4H, s, Ar-C**H**$_2$-N & ArCN-C**H**2-N), 7.39 – 7.60 (9H, m, arene-**H**), 7.63 – 7.94 (8H, m, benzimi-**H**), 10.14 (1H, s, ArCH$_2$NC**H**N), 10.21 (1H, s, NC**H**NCH$_2$ArCN). **^{13}C NMR** (125 MHz, d_6-DMSO) in δ ppm: 45.97, 46.26 (N-**C**H$_2$**C**H$_2$-N), 50.55 (ArCN-**C**H$_2$-N), 50.58 (Ar-**C**H$_2$-N), 114.46 (C≡N), 126.44, 126.52, 127.03, 127.29, 128.34, 128.97, 129.51, 130.21, 131.34, 132.56, 133.05, 133.35, 133.93 (arene-**C**/benzimi-**C**), 143.70 (ArCH$_2$N**C**HN), 143.81 (N**C**HNCH$_2$ArCN). Anal. Calc. for C$_{31}$H$_{27}$N$_5$Br$_2$: C, 79.29; H, 5.80; N, 14.91%. Found: C, 78.66; H, 5.45; N, 13.99%

N,N'-(ethane-1,2-diyl)-1-benzylbenzimidazolium-1'-(3-benzonitrile)benzimidazolium dibromide, 2Br

White solid (powder). **Yield**: 1.24 g (74 %), **MP**: 240 - 244 °C. **FTIR** (ATR, cm^{-1}): 3029 (Csp^3-H$_{arom}$ stretching); 2960 (Csp^3-H$_{aliphatic}$ stretching); 2236 (C≡N stretching); 1455 (C-N stretching). **^{1}H NMR** (500 MHz, *d$_6$*-DMSO) in δ ppm: 5.20 (4H, s, N-C**H**$_2$C**H**$_2$-N), 5.75 (4H, s, Ar-C**H**$_2$-N & ArCN-C**H**$_2$-N), 7.37 – 7.49 (9H, m, arene-**H**), 7.63 – 7.97 (8H, m, benzimi-**H**), 10.17 (1H, s, ArCH$_2$NC**H**N), 10.22 (1H, s, NC**H**NCH$_2$ArCN). **^{13}C NMR** (125 MHz, *d$_6$*-DMSO) in δ ppm: 46.16, 46.40 (N-**C**H$_2$**C**H$_2$-N), 50.54 (ArCN-**C**H$_2$-N), 50.56 (Ar-**C**H$_2$-N), 114.40 (**C**≡N), 125.24, 125.73, 126.54, 127.01, 127.45, 128.03, 129.67, 131.22, 132.98, 133.54 (arene-**C**/benzimi-**C**), 143.67 (ArCH$_2$N**C**HN), 143.88 (N**C**HNCH$_2$ArCN). Anal. Calc. for C$_{31}$H$_{27}$N$_5$Br$_2$: C, 79.29; H, 5.80; N, 14.91%. Found: C, 78.06; H, 4.92; N, 14.57%

N,N'-(ethane-1,2-diyl)-1-benzylbenzimidazolium-1'-(4-benzonitrile)benzimidazolium dibromide, 3Br

White solid (powder). **Yield**: 1.20 g (75 %), **MP**: 243 - 245 °C. **FTIR** (ATR, cm^{-1}): 3028 (Csp^3-H$_{arom}$ stretching); 2964 (Csp^3-H$_{aliphatic}$ stretching); 2232 (C≡N stretching); 1454 (C-N stretching). **^{1}H NMR** (500 MHz, *d$_6$*-DMSO) in δ ppm: 5.24 (4H, s, N-C**H**$_2$C**H**$_2$-N), 5.78 (4H, s, Ar-C**H**2-N & ArCN-C**H**2-N), 7.39 – 7.60 (9H, m, arene-**H**), 7.63 – 7.94 (8H, m, benzimi-**H**), 10.14 (1H, s, ArCH$_2$NC**H**N), 10.21 (1H, s, NC**H**NCH$_2$ArCN). **^{13}C NMR** (125 MHz, *d$_6$*-DMSO) in δ ppm: 46.13, 46.34 (N-**C**H$_2$**C**H$_2$-N), 50.18 (ArCN-**C**H$_2$-N), 50.57 (Ar-**C**H$_2$-N), 114.46 (**C**≡N), 127.26, 127.34, 128.52, 128.69, 128.86, 129.44, 131.10, 131.27, 131.63, 134.06, 137.04 (arene-**C**/benzimi-**C**), 143.70 (ArCH$_2$N**C**HN), 143.88 (N**C**HNCH$_2$ArCN). Anal. Calc. for C$_{31}$H$_{27}$N$_5$Br$_2$: C, 79.29; H, 5.80; N, 14.91%. Found: C, 78.77; H, 5.30; N, 14.56%

General procedure for the synthesis of N,N'-(propane-1,2-diyl)-1-benzylbenzimidazolium-1'-(n-benzonitrile)benzimidazolium dibromide, (4Br – 6Br) (n = 2, 3 & 4) derivatives

The *N*-(2-(bromomethyl)benzonitrile)benzimidzole (0.57 g, 2.44 mmol) was added to the synthesized *N*-(2-bromopropyl)-*N'*-benzylbenzimidazolium bromide, **ii·Br** (1.00 g, 2.44 mmol) dissolved in acetonitrile (20 mL) and the reaction mixture was refluxed for 24 h at 80 –

100 °C. Upon cooling at room temperature, a sticky-brown precipitate formed then filtered and washed with acetonitrile (5 mL) and diethyl ether (2 × 3 mL). Bromide salt was used for further synthesis, whereas the hexafluorophosphate salt was used for characterization purposes. The bromide salt was converted into hexafluorophosphate counterion by metathesis reaction using KPF_6 (0.13 g, 1.00 mmol) in methanol (20 mL). The mixture was stirred for 3 h, filtered and washed with distilled water (3 x 2 mL) and then recrystallize from acetonitrile/diethyl ether.

N,N'-(propane-1,2-diyl)-1-benzylbenzimidazolium-1'-(n-benzonitrile)benzimidazolium dibromide, 4Br and 4PF₆

Brown solid (powder). **Yield**: 1.09 g (70 %), **MP**: 268 - 269 °C. **FTIR** (ATR, cm^{-1}): 3024 (Csp^3-H$_{arom}$ stretching); 2926 (Csp^3-H$_{aliphatic}$ stretching); 2230 (C≡N stretching); 1453 (C-N stretching). **¹H NMR** (500 MHz, *d₆*-DMSO) in δ ppm: 4.72 (2H, d, N-CH$_2$C**H**$_2$CH$_2$-N, *J* = 25 Hz), 5.77 (4H, s, N-C**H**$_2$CH$_2$C**H**$_2$-N), 6.03 (4H, s, Ar-C**H**$_2$-N & N-C**H**$_2$-ArCN), 7.41 – 7.75 (9H, m, arene-**H**), 7.89 – 8.16 (8H, m, benzimi-**H**), 9.84 (1H, s, ArCH$_2$NC**H**N), 9.86 (1H, s, NC**H**NCH$_2$ArCN). **¹³C NMR** (125 MHz, *d₆*-DMSO) in δ ppm: 28.53, 31.10, 44.56 (N-**C**H$_2$**C**H$_2$**C**H$_2$-N), 49.04 (Ar-**C**H$_2$-N), 50.48 (N-**C**H$_2$-ArCN), 114.39 (**C**≡N), 111.36, 117.44, 127.24, 127.42, 128.62, 129.25, 129.47, 129.66, 130.11, 131.44, 131.66, 131.83, 134.24, 134.46, 137.21 (arene-**C**/benzimi-**C**), 142.97 (ArCH$_2$N**C**HN), 143.82 (N**C**HNCH$_2$ArCN). Anal. Calc. for $C_{32}H_{29}N_5Br_2$: C, 79.47; H, 6.04; N, 14.48%. Found: C, 78.95; H, 5.54; N, 14.13%

N,N'-(propane-1,2-diyl)-1-benzylbenzimidazolium-1'-(3-benzonitrile)benzimidazolium dibromide, 5Br and 5PF₆

Greyish solid (powder). **Yield**: 1.12 g (73 %), **MP**: 269 - 271 °C. **FTIR** (ATR, cm^{-1}): 3100 (Csp^3-H$_{arom}$ stretching); 2934 (Csp^3-H$_{aliphatic}$ stretching); 2227 (C≡N stretching); 1446 (C-N stretching). **¹³C NMR** (125 MHz, *d₆*-DMSO) in δ ppm: 28.48, 31.80, 44.61 (N-**C**H$_2$**C**H$_2$**C**H$_2$-N), 46.05 (Ar-**C**H$_2$-N), 47.05 (N-**C**H$_2$-ArCN) 114.41 (**C**≡N), 127.24, 127.34, 128.73, 129.26, 131.43, 131.83, 134.29 (arene-**C**/benzimi-**C**), 143.01 (ArCH$_2$N**C**HN), 143.05 (N**C**HNCH$_2$ArCN). Anal. Calc. for $C_{32}H_{29}N_5Br_2$: C, 79.47; H, 6.04; N, 14.48%. Found: C, 79.06; H, 5.57; N, 14.03%

*‡The ^{1}H-NMR of bis-benzimidazolium salt of **5PF₆** showing the broadening of the signal as it appeared to be high flexibility of bis-benzimidazolium salt structure.*

N,N'-(propane-1,2-diyl)-1-benzylbenzimidazolium-1'-(4-benzonitrile)benzimidazolium dibromide, 6Br and 6PF₆

Greyish solid (powder). **Yield**: 1.12 g (71 %), **MP**: 270 - 272 °C. **FTIR** (ATR, cm^{-1}): 3096 (Csp^3-H$_{arom}$ stretching); 2940 (Csp^3-H$_{aliphatic}$ stretching); 2231 (C≡N stretching); 1445 (C-N stretching). **^{13}C NMR** (125 MHz, d_6-DMSO) in δ ppm: 28.62, 32.01, 44.55 (N-**C**H$_2$**C**H$_2$**C**H$_2$-N), 44.07 (Ar-**C**H$_2$-N), 45.69 (N-**C**H$_2$-ArCN) 114.29 (C≡N), 126.97, 127.56, 129.05, 129.99, 131.05, 131.64, 131.89, 132.06 (arene-**C**/benzimi-**C**), 143.29 (ArCH$_2$N**C**HN), 143.37 (N**C**HNCH$_2$ArCN). Anal. Calc. for C$_{32}$H$_{29}$N$_5$Br$_2$: C, 79.47; H, 6.04; N, 14.48%. Found: C, 78.93; H, 6.32; N, 13.99%

*‡The ^{1}H-NMR of bis-benzimidazolium salt of **6PF₆** showing the broadening of the signal as it appeared to be high flexibility of the bis-benzimidazolium salt structure.*

General procedure for the synthesis of N,N'-(butane-1,2-diyl)-1-benzylbenzimidazolium-1'-(n-benzonitrile)benzimidazolium dibromide, (7Br – 9Br) (n = 2, 3 & 4) derivatives

The *N*-(2-(bromomethyl)benzonitrile)benzimidazole (0.55 g, 2.34 mmol) was added to the synthesized *N*-(2-bromobutyl)-*N*'-benzylbenzimidazolium bromide, **iii·Br** (1.00 g, 2.36 mmol) dissolved in acetonitrile (20 mL) and the reaction mixture was refluxed for 24 h at 80 – 100 °C. Upon cooling at room temperature, a sticky brown precipitate formed then filtered and washed with acetonitrile (5 mL) and diethyl ether (2 × 3 mL). Bromide salt was used for further synthesis, whereas the hexafluorophosphate salt was used for characterization purposes. The bromide salt was converted into hexafluorophosphate counterion by metathesis reaction using KPF$_6$ (0.13 g, 1.00 mmol) in methanol (10 mL). The mixture was stirred for 3 h, filtered and washed with distilled water (3 x 2 mL) and then recrystallize from acetonitrile/diethyl ether.

N,N'-(butane-1,2-diyl)-1-benzylbenzimidazolium-1'-(2-benzonitrile)benzimidazolium
dibromide, 7Br and 7PF$_6$

Brown solid (powder). **Yield**: 1.13 g (73 %), **MP**: 281 - 283 °C. **FTIR** (ATR, cm^{-1}): 3103 (Csp^3-H$_{arom}$ stretching); 2967 (Csp^3-H$_{aliphatic}$ stretching); 2227 (C≡N stretching); 1455 (C-N stretching). **^{1}H NMR** (500 MHz, *d$_6$*-DMSO) in δ ppm: 4.61 (4H, s, N-CH$_2$C**H**$_2$C**H**$_2$CH$_2$-N), 5.77 (4H, s, N-C**H**$_2$CH$_2$CH$_2$C**H**$_2$-N), 6.02 (4H, s, Ar-C**H**2-N & ArCN-C**H**$_2$-N), 7.38 – 7.70 (9H, m, arene-**H**), 7.72 – 8.16 (8H, m, benzimi-**H**), 9.84 (1H, s, ArCH$_2$NC**H**N), 9.87 (1H, s, NC**H**NCH$_2$ArCN). **^{13}C NMR** (125 MHz, *d$_6$*-DMSO) in δ ppm: 26.01, 26.09, 46.75, 46.83 (N-**C**H$_2$**C**H$_2$**C**H$_2$**C**H$_2$-N), 49.07 (Ar-**C**H$_2$-N), 50.41 (N-**C**H$_2$-ArCN), 114.38 (**C**≡N), 111.32, 117.41, 127.19, 127.30, 127.57, 128.67, 129.48, 129.76, 130.13, 131.61, 131.75, 134.39, 134.49, 137.25 (arene-**C**/benzimi-**C**), 142.86 (ArCH$_2$N**C**HN), 143.75 (N**C**HNCH$_2$ArCN). Anal. Calc. for C$_{33}$H$_{31}$N$_5$P$_2$F$_{12}$: C, 79.65; H, 6.28; N, 14.07%. Found: C, 79.13; H, 5.78; N, 13.72%

N,N'-(butane-1,2-diyl)-1-benzylbenzimidazolium-1'-(3-benzonitrile)benzimidazolium
dibromide, 8Br and 8PF$_6$

White solid (powder). **Yield**: 1.15 g (74 %), **MP**: 282 - 284 °C. **FTIR** (ATR, cm^{-1}): 3096 (Csp^3-H$_{arom}$ stretching); 2957 (Csp^3-H$_{aliphatic}$ stretching); 2239 (C≡N stretching); 1456 (C-N stretching). **^{1}H NMR** (500 MHz, *d$_6$*-DMSO) in δ ppm: 4.59 (4H, s, N-CH$_2$C**H**$_2$C**H**$_2$CH$_2$-N), 5.77 (4H, s, N-C**H**$_2$CH$_2$CH$_2$C**H**$_2$-N), 5.82 (4H, s, Ar-C**H**2-N & ArCN-C**H**2-N), 7.40 – 7.70 (9H, m, arene-**H**), 7.85 – 8.12 (8H, m, benzimi-**H**), 9.86 (1H, s, ArCH$_2$NC**H**N), 9.88 (1H, s, NC**H**NCH$_2$ArCN). **^{13}C NMR** (125 MHz, *d$_6$*-DMSO) in δ ppm: 25.99, 26.04, 46.80, 46.84 (N-**C**H$_2$**C**H$_2$**C**H$_2$**C**H$_2$-N), 49.49 (ArCN-**C**H$_2$-N), 50.41 (Ar-**C**H$_2$-N), 114.32 (**C**≡N), 127.19, 127.22, 127.38, 128.67, 129.24, 129.48, 130.65, 131.33, 131.41, 132.35, 132.99, 133.63, 134.37, 135.94 (arene-**C**/benzimi-**C**), 142.89 (ArCH$_2$N**C**HN), 143.27 (N**C**HNCH$_2$ArCN). Anal. Calc. for C$_{33}$H$_{31}$N$_5$P$_2$F$_{12}$: C, 79.65; H, 6.28; N, 14.07%. Found: C, 79.24; H, 5.81; N, 13.62%

N,N'-(butane-1,2-diyl)-1-benzylbenzimidazolium-1'-(3-benzonitrile)benzimidazolium dibromide, 9Br and 9PF$_6$

White solid (powder). **Yield**: 1.15 g (74 %), **MP**: 284 - 286 °C. **FTIR** (ATR, cm^{-1}): 3099 (Csp^3-H$_{arom}$ stretching); 2932 (Csp^3-H$_{aliphatic}$ stretching); 2236 (C≡N stretching); 1446 (C-N stretching). **^{1}H NMR** (500 MHz, *d$_6$*-DMSO) in δ ppm: 4.56 (4H, s, N-CH$_2$C**H**$_2$C**H**$_2$CH$_2$-N), 4.68 (4H, s, N-C**H**$_2$CH$_2$CH$_2$C**H**$_2$-N), 5.74 (4H, s, Ar-C**H**$_2$-N & N-C**H**$_2$-ArCN), 7.39 – 7.68 (9H, m, arene-**H**), 7.93 – 8.06 (8H, m, benzimi-**H**), 9.69 (1H, s, ArCH$_2$NC**H**N), 9.85 (1H, s, NC**H**NCH$_2$ArCN). **^{13}C NMR** (125 MHz, *d$_6$*-DMSO) in δ ppm: 26.00, 30.94, 46.63, 46.77 (N-**C**H$_2$**C**H$_2$**C**H$_2$**C**H$_2$-N), 50.43 (Ar-**C**H$_2$-N), 50.50 (N-**C**H$_2$-ArCN), 114.31 (C≡N), 127.21, 127.30,128.70, 129.49, 131.34, 13171, 134.31 (arene-**C**/benzimi-**C**), 142.84 (ArCH$_2$N**C**HN), 143.35 (N**C**HNCH$_2$ArCN). Anal. Calc. for C$_{33}$H$_{31}$N$_5$P$_2$F$_{12}$: C, 79.65; H, 6.28; N, 14.07%. Found: C, 79.16; H, 6.78; N, 13.65%

General procedure for the synthesis of [Bis(N,N'-(ethane/propane/butane-1,2-diyl)-1-benzylbenzimidazolium-1'-(2-benzonitrile)benzimidazolium)disilver(I)] dihexafluorophosphate, (Ag1 – Ag9) (n = 2, 3 & 4) derivatives

A mixture of salt **1Br** (0.30 g, 0.48 mmol) and Ag$_2$O (0.22 g, 0.95 mmol) in methanol (15 mL) was stirred at room temperature for 48 h and covered with aluminium foil to avoid light. The reaction mixture was filtered through a pad of Celite to remove unreacted silver. The colorless filtrate then was subjected into hexafluorophosphate counterion by metathesis reaction using KPF$_6$ (0.18 g, 0.98 mmol) in methanol. The mixture was stirred at room temperature for 3 h and allowed to stand overnight. Then, the mixture was filtered through filter paper and washed with distilled water (2 x 3 mL) and air-dried before recrystallized using acetonitrile (20 mL) and diethyl ether (100 mL) to afford the silver(I) di-NHC complex.

[Bis(N,N'-(ethane-1,2-diyl)-1-benzylbenzimidazolium-1'-(2-benzonitrile)benzimidazolium)disilver(I)] dihexafluorophosphate, Ag1

Greyish powder (solid). **Yield**: 0.42 g (60 %), **MP**: 261 - 264 °C. **FTIR** (ATR, cm^{-1}): 3021 (Csp^3-H$_{arom}$ stretching); 2932 (Csp^3-H$_{aliphatic}$ stretching); 2238 (C≡N stretching); 1450 (C-N stretching). **^{1}H NMR** (500 MHz, *d$_6$*-DMSO) in δ ppm: 5.32 (8H, s, N-C**H**$_2$C**H**$_2$-N), 5.59 (8H,

s, Ar-C**H**$_2$-N & N-C**H**$_2$-ArCN), 6.77 – 7.38 (9H, m, arene-**H**), 7.47 – 7.93 (8H, m, benzimi-**H**). **^{13}C NMR** (125 MHz, d_6-DMSO) in δ ppm: 46.30, 47.29 (N-**C**H$_2$**C**H$_2$-N), 51.03 (Ar-**C**H$_2$-N), 51.37 (N-**C**H$_2$-ArCN), 112.34 (C≡N), 123.56, 123.99, 124.00, 124.45, 125.36, 127.25, 128.54, 128.91, 130.22, 131.01, 132.76, 133.23 (arene-**C**/benzimi-**C**), 189.75, 190.22 (**C**$_{carbene}$-Ag). Anal. Calc. for C$_{62}$H$_{54}$Ag$_2$N$_{10}$P$_2$F$_{12}$: C, 64.48; H, 4.71; N, 12.13%. Found: C, 63.82; H, 4.20; N, 13.10%

[Bis(N,N'-(ethane-1,2-diyl)-1-benzylbenzimidazolium-1'-(3-benzonitrile)benzimidazolium)disilver(I)] dihexafluorophosphate, Ag2

Brown solid (powder). **Yield**: 0.41 g (58 %), **MP**: 262 - 265 °C. **FTIR** (ATR, cm^{-1}): 3030 (Csp^3-H$_{arom}$ stretching); 2919 (Csp^3-H$_{aliphatic}$ stretching); 2237 (C≡N stretching); 1443 (C-N stretching). **^{1}H NMR** (500 MHz, d_6-DMSO) in δ ppm: 5.29 (8H, s, N-C**H**$_2$C**H**$_2$-N), 5.54 (8H, s, Ar-C**H**$_2$-N & N-C**H**$_2$-ArCN), 6.76 – 7.36 (9H, m, arene-**H**), 7.45 – 7.92 (8H, m, benzimi-**H**). **^{13}C NMR** (125 MHz, d_6-DMSO) in δ ppm: 46.58, 48.03 (N-**C**H$_2$**C**H$_2$-N), 50.46 (Ar-**C**H$_2$-N), 51.55 (N-**C**H$_2$-ArCN), 112.89 (C≡N), 124.05, 124.56, 125.21, 125.40, 125.98, 126.23, 126.78, 127.89, 128.29, 128.45, 130.21, 131.44, 132.67, 133.24 (arene-**C**/benzimi-**C**), 190.31, 192.34 (**C**$_{carbene}$-Ag). Anal. Calc. for C$_{62}$H$_{54}$Ag$_2$N$_{10}$P$_2$F$_{12}$: C, 64.48; H, 4.71; N, 12.13%. Found: C, 65.26; H, 5.09; N, 13.22%

[Bis(N,N'-(ethane-1,2-diyl)-1-benzylbenzimidazolium-1'-(4-benzonitrile)benzimidazolium)disilver(I)] dihexafluorophosphate, Ag3

Brown solid (powder). **Yield**: 0.39 g (57 %), **MP**: 263 - 265 °C. **FTIR** (ATR, cm^{-1}): 3023 (Csp^3-H$_{arom}$ stretching); 2925 (Csp^3-H$_{aliphatic}$ stretching); 2236 (C≡N stretching); 1446 (C-N stretching). **^{1}H NMR** (500 MHz, d_6-DMSO) in δ ppm: 5.30 (8H, s, N-C**H**$_2$C**H**$_2$-N), 5.51 (8H, s, Ar-C**H**$_2$-N & N-C**H**$_2$-ArCN), 6.74 – 7.33 (9H, m, arene-**H**), 7.40 – 7.89 (8H, m, benzimi-**H**). **^{13}C NMR** (125 MHz, d_6-DMSO) in δ ppm: 46.73, 47.25 (N-**C**H$_2$**C**H$_2$-N), 50.98 (Ar-**C**H$_2$-N), 51.35 (N-**C**H$_2$-ArCN), 111.87 (C≡N), 123.70, 123.97, 125.68, 127.23, 127.47, 128.05, 128.33, 132.30, 132.87, 133.25, 135.06 (arene-**C**/benzimi-**C**), 192.70, 195.90 (**C**$_{carbene}$-Ag). Anal. Calc. for C$_{62}$H$_{54}$Ag$_2$N$_{10}$P$_2$F$_{12}$: C, 64.48; H, 4.71; N, 12.13%. Found: C, 63.96; H, 5.21; N, 11.78%

[Bis(N,N'-(propane-1,2-diyl)-1-benzylbenzimidazolium-1'-(2-benzonitrile)benzimidazolium)disilver(I)] dihexafluorophosphate, Ag4

Brown solid (powder). **Yield**: 0.40 g (58 %), **MP**: 278 - 280 °C. **FTIR** (ATR, cm^1): 2953 (Csp^3-H$_{arom}$ stretching); 2850 (Csp^3-H$_{aliphatic}$ stretching); 2225 (C≡N stretching); 1442 (C-N stretching). **^{13}C NMR** (125 MHz, d_6-DMSO) in δ ppm: 46.77, 46.92, 47.02 (N-**C**H$_2$**C**H$_2$**C**H$_2$-N), 50.70 (Ar-**C**H$_2$-N), 52.12 (N-**C**H$_2$-ArCN), 112.49 (C≡N), 124.89, 124.97, 125.09, 125.19, 128.38, 129.10, 129.27, 133.65, 134.12 (arene-**C**/benzimi-**C**), 170.89 (**C**$_{carbene}$-Ag). Anal. Calc. for C$_{64}$H$_{58}$Ag$_2$N$_{10}$P$_2$F$_{12}$: C, 64.98; H, 4.94; N, 11.84%. Found: C, 65.39; H, 4.47; N, 12.29%

‡ *The ^{1}H-NMR of Ag(I) di-NHC complex of* **Ag4** *showing the broadening of the signal as it appeared to be high fluxionality of the complex structure.*

[Bis(N,N'-(propane-1,2-diyl)-1-benzylbenzimidazolium-1'-(3-benzonitrile)benzimidazolium)disilver(I)] dihexafluorophosphate, Ag5

Greyish solid (powder). **Yield**: 0.40 g (58 %), **MP**: 279 - 281 °C. **FTIR** (ATR, cm^{-1}): 2922 (Csp^3-H$_{arom}$ stretching); 2823 (Csp^3-H$_{aliphatic}$ stretching); 2239 (C≡N stretching); 1453 (C-N stretching). **^{1}H NMR** (500 MHz, d_6-DMSO) in δ ppm: 4.68 (4H, d, N-CH$_2$C**H**$_2$CH$_2$-N, J = 6.2 Hz), 5.66 (8H, s, N-C**H**$_2$CH$_2$C**H**$_2$-N), 5.79 (8H, s, Ar-C**H**$_2$-N & N-C**H**$_2$-ArCN), 7.10 – 7.48 (9H, m, arene-**H**), 7.74 – 7.85 (8H, m, benzimi-**H**). **^{13}C NMR** (125 MHz, d_6-DMSO) in δ ppm: 46.40, 47.09, 51.20 (N-**C**H$_2$**C**H$_2$**C**H$_2$-N), 52.16 (Ar-**C**H$_2$-N), 52.29 (N-**C**H$_2$-ArCN), 112.96 (C≡N), 124.70, 124.89, 127.15, 125.62, 128.35, 128.64, 129.29, 129.46, 133.78, 133.96 (arene-**C**/benzimi-**C**), 188.22, 190.78 (**C**$_{carbene}$-Ag). Anal. Calc. for C$_{64}$H$_{58}$Ag$_2$N$_{10}$P$_2$F$_{12}$: C, 64.98; H, 4.94; N, 11.84%. Found: C, 64.46; H, 5.44; N, 11.49%

[Bis(N,N'-(propane-1,2-diyl)-1-benzylbenzimidazolium-1'-(4-benzonitrile)benzimidazolium)disilver(I)] dihexafluorophosphate, Ag6

Brown powder (solid). **Yield**: 0.41 g (60 %), **MP**: 280 - 282 °C. **FTIR** (ATR, cm^1): 2920 (Csp^3-H$_{arom}$ stretching); 2832 (Csp^3-H$_{aliphatic}$ stretching); 2240 (C≡N stretching); 1459 (C-N stretching). **^{13}C NMR** (125 MHz, d_6-DMSO) in δ ppm: 46.56, 47.37, 51.70 (N-**C**H$_2$**C**H$_2$**C**H$_2$-

N), 52.76 (Ar-$\underline{C}$H$_2$-N), 52.89 (N-$\underline{C}$H$_2$-ArCN), 112.23 (C≡N), 124.39, 124.87, 126.49, 127.19, 128.68, 129.10, 130.27, 131.19, 131.34, 131.70, 133.65, 134.12 (arene-$\underline{C}$/benzimi-$\underline{C}$), 182.45, 186.29 ($\underline{C}$$_{carbene}$-Ag). Anal. Calc. for C$_{64}H_{58}Ag_2N_{10}P_2F_{12}$: C, 64.98; H, 4.94; N, 11.84%. Found: C, 65.56; H, 4.32; N, 12.21%

*‡ The ¹H-NMR of Ag(I) di-NHC complex of **Ag6** showing the broadening of the signal as it is appeared to be high fluxionality of the complex structure.*

[Bis(N,N'-(butane-1,2-diyl)-1-benzylbenzimidazolium-1'-(2-benzonitrile)benzimidazolium)disilver(I)] dihexafluorophosphate, Ag7

Greyish solid (powder). **Yield**: 0.38 g (55 %), **MP**: 297 - 299 °C. **FTIR** (ATR, cm^{-1}): 2926 (Csp^3-H$_{arom}$ stretching); 2843 (Csp^3-H$_{aliphatic}$ stretching); 2224 (C≡N stretching); 1450 (C-N stretching). **¹H NMR** (500 MHz, d_6-DMSO) in δ ppm: 4.58 (8H, s, N-CH$_2$C$\underline{H}$$_2C\underline{H}$$_2CH_2$-N), 5.67 (8H, s, N-C$\underline{H}$$_2CH_2CH_2C\underline{H}$$_2$-N), 5.92 (8H, s, Ar-C$\underline{H}$$_2$-N & N-C$\underline{H}$$_2$-ArCN), 7.04 – 7.48 (9H, m, arene-$\underline{H}$), 7.50 – 7.88 (8H, m, benzimi-$\underline{H}$). **¹³C NMR** (125 MHz, d_6-DMSO) in δ ppm: 46.66, 49.05, 50.83, 51.98 (N-$\underline{C}$H$_2$$\underline{C}H_2$$\underline{C}H_2$$\underline{C}H_2$-N), 53.45 (Ar-$\underline{C}H_2$-N), 58.26 (N-$\underline{C}H_2$-ArCN), 112.90 (C≡N), 124.79, 124.96, 127.46, 128.28, 128.69, 129.07, 129.26, 129.47, 133.88, 133.99 (arene-$\underline{C}$/benzimi-$\underline{C}$), 188.89, 194.83 ($\underline{C}$$_{carbene}$-Ag). Anal. Calc. for C$_{66}H_{62}Ag_2N_{10}P_2F_{12}$: C, 65.46; H, 5.16; N, 11.57%. Found: C, 65.87; H, 4.69; N, 12.02%

[Bis(N,N'-(butane-1,2-diyl)-1-benzylbenzimidazolium-1'-(3-benzonitrile)benzimidazolium)disilver(I)] dihexafluorophosphate, Ag8

Greyish solid (powder). **Yield**: 0.39 g (57 %), **MP**: 298 - 300 °C. **FTIR** (ATR, cm^{-1}): 2925 (Csp^3-H$_{arom}$ stretching); 2827 (Csp^3-H$_{aliphatic}$ stretching); 2225 (C≡N stretching); 1449 (C-N stretching). **¹H NMR** (500 MHz, d_6-DMSO) in δ ppm: 4.57 (8H, s, N-CH$_2$C$\underline{H}$$_2C\underline{H}$$_2CH_2$-N), 5.67 (8H, s, N-C$\underline{H}$$_2CH_2CH_2C\underline{H}$$_2$-N), 5.73 (8H, s, Ar-C$\underline{H}$$_2$-N & N-C$\underline{H}$$_2$-ArCN), 7.07 – 7.47 (9H, m, arene-$\underline{H}$), 7.69 – 7.84 (8H, m, benzimi-$\underline{H}$). **¹³C NMR** (125 MHz, d_6-DMSO) in δ ppm: 47.53, 48.94, 51.20, 52.00 (N-$\underline{C}$H$_2$$\underline{C}H_2$$\underline{C}H_2$$\underline{C}H_2$-N), 53.43 (Ar-$\underline{C}H_2$-N), 58.24 (N-$\underline{C}H_2$-ArCN), 112.91 (C≡N), 124.96, 127.46, 128.28, 128.69, 129.07, 129.21, 129.26, 129.47, 133.8, 133.99 (arene-$\underline{C}$/benzimi-$\underline{C}$), 189.05, 189.75 ($\underline{C}$$_{carbene}$-Ag). Anal. Calc. for C$_{66}H_{62}Ag_2N_{10}P_2F_{12}$: C, 65.46; H, 5.16; N, 11.57%. Found: C, 64.94; H, 5.66; N, 11.22%.

[Bis(N,N'-(butane-1,2-diyl)-1-benzylbenzimidazolium-1'-(4-benzonitrile)benzimidazolium)disilver(I)] dihexafluorophosphate, Ag9

Brown solid (powder). **Yield**: 0.40 g (58 %), **MP**: 300 - 302 °C. **FTIR** (ATR, cm^{-1}): 2926 (Csp^3-H$_{arom}$ stretching); 2827 (Csp^3-H$_{aliphatic}$ stretching); 2224 (C≡N stretching); 1450 (C-N stretching). **^{1}H NMR** (500 MHz, *d$_6$*-DMSO) in δ ppm: 4.57 (8H, s, N-CH$_2$C**H**$_2$C**H**$_2$CH$_2$-N), 4.69 (8H, s, N-C**H**$_2$CH$_2$CH$_2$C**H**$_2$-N), 5.69 (8H, s, Ar-C**H**$_2$-N & N-C**H**$_2$-ArCN), 7.13 – 7.46 (9H, m, arene-**H**), 7.73 – 7.84 (8H, m, benzimi-**H**). **^{13}C NMR** (125 MHz, *d$_6$*-DMSO) in δ ppm: 46.89, 48.65, 48.96, 52.00 (N-**C**H$_2$**C**H$_2$**C**H$_2$**C**H$_2$-N), 52.18 (Ar-**C**H$_2$-N), 59.61 (N-**C**H$_2$-ArCN), 112.90 (C≡N), 124.82, 126.99, 127.47, 127.63, 127.93, 128.39, 129.10, 129.17, 133.89 (arene-**C**/benzimi-**C**), 176.80, 177.03 (**C**$_{carbene}$-Ag). Anal. Calc. for C$_{66}$H$_{62}$Ag$_2$N$_{10}$P$_2$F$_{12}$: C, 65.46; H, 5.16; N, 11.57%. Found: C, 64.94; H, 5.66; N, 11.22%

The data pre-processing

The ^{1}H- and ^{13}C-NMR spectra were converted and transferred as .xlsx format using Microsoft Excel and imported to the dataset table in XLSTAT (2024 version) software [14]. Next, the Kaiser-Meyer-Olkin (KMO) test verified dataset adequacy and proceeded with the principal component analysis (PCA) to find the correlation of the ^{1}H- and ^{13}C NMR results data.

The Kaiser-Meyer-Olkin (KMO) test

The dataset was analysed for dataset adequacy by the KMO test. An adequate dataset determines the ability to generated model to extract latent variables from the dataset. In this study, the KMO test was employed at significant level, α = 0.01. The calculated KMO was ranked as KMO < 0.5 = inadequate, 0.5 < KMO < 0.7 = mediocre, 0.7 < KMO < 0.8 = good, 0.8 < KMO < 0.9 = very good and KMO > 0.9 = excellent to indicate the dataset adequacy [15].

The dataset transformation

To ensure that the dataset followed a normal distribution before the PCA, the dataset normality was tested using Shapiro-Wilk test at $\alpha = 0.01$. The dataset was transformed using standard deviation (n-1) method.

The principal component analysis (PCA)

The ^{1}H- and ^{13}C-NMR spectra was extracted its ppm value to obtain dataset for PCA. The ^{1}H- and ^{13}C-NMR spectra at the baseline of δ 0 – 11 ppm for ^{1}H-NMR as well δ 0 – 200 for ^{13}C-NMR, respectively. Analysis of PCA was performed using XLSTAT software, and the data were scaled using Pareto scaling technique prior to PCA analysis to maximize the variation. After Pareto scaling, the variables used for PCA model were more normally distributed shown by its Gaussian curve. The number of principal components (PCs) was optimized to obtain optimum differentiation among samples. The differentiation result of samples was observed using PCA score plot. Moreover, PCA model was evaluated using its R^2 and Q^2 value to justify the good of fitness and predictivity of the PCA model, respectively [16].

RESULTS AND DISCUSSIONS

The Synthesis

The synthesis started with the *N*-arylation (aryl = benzyl, 2-methylbenzonitrile, 3-methylbenzonitrile and 4-methylbenzonitrile) to the benzimidazole ring. The precursors consisting of linked system of *N*-(2-bromoethyl)-*N'*-benzylbenzimidazolium bromide, **i·Br**, *N*-(2-bromopropyl)-*N'*-benzylbenzimidazolium bromide, **ii·Br**, and *N*-(2-bromobutyl)-*N'*-benzylbenzimidazolium bromide, **iii·Br**, were synthesized by the reaction between *n*-benzylbenzimidazole with excess 1,2/3/4-dibromoethane/propane/butane in neat. The products obtained consisting of white precipitate, and brown precipitate in relatively appreciable yield.

The synthesized nitrile-functionalized bis-benzimidazolium salts, **1Br** – **9Br**, were done by reacting an equimolar *N*-(*n*-(bromomethyl)benzonitrile)benzimidazole (where *n* = 2, 3 and 4) with *N*-(2-bromoethyl)-*N'*-benzylbenzimidazolium bromide, **i·Br**, *N*-(2-bromopropyl)-*N'*-

benzylbenzimidazolium bromide, **ii·Br**, and *N*-(2-bromobutyl)-*N*'-benzylbenzimidazolium bromide, **iii·Br**, in acetonitrile as shown in **Scheme 1**. For ease of characterization and purification purposes, the bis-benzimidazolium dibromide salts of **1Br – 9Br**, were converted to their respective dihexafluorophosphate counterions of **4PF₆ – 9PF₆**. All the dihexafluorophosphate salts are stable to air and moisture as well, soluble in common organic solvents such as acetonitrile, DMSO, methanol, dichloromethane, DMF and acetone as compared to their respective bromide salts that are partially soluble.
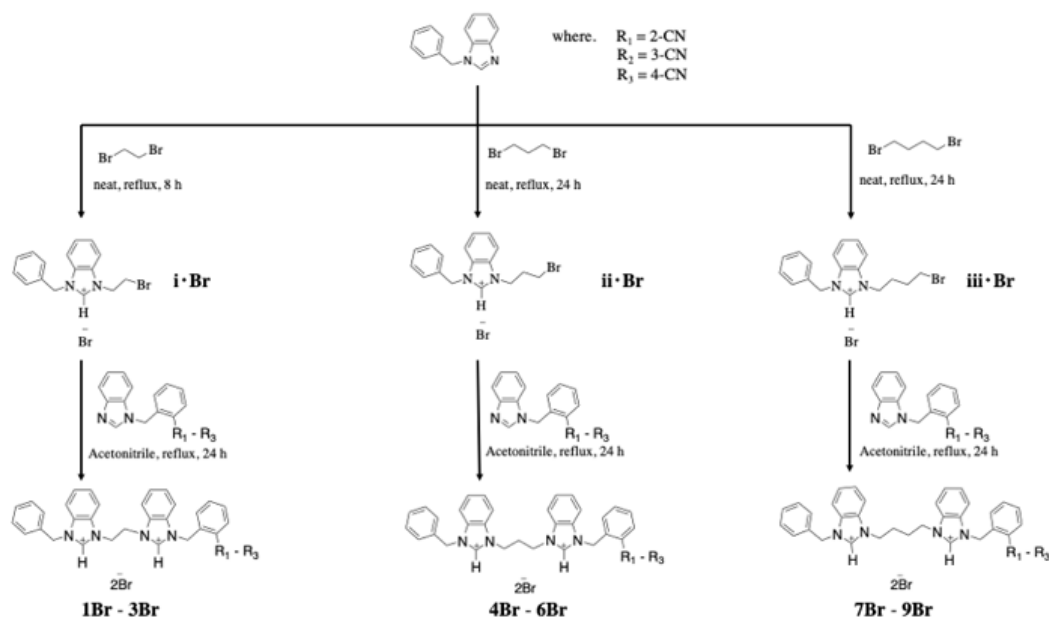
Scheme 1. The schematic diagram formation of nitrile functionalized bis-benzimidazolium salts (**1Br – 9Br**) varying different alkane bridges of ethylene/propylene/butylene.

Furthermore, the silver(I) di-NHC complexes, **Ag1 – Ag9** were synthesized by *in-situ* deprotonation of all the bis-benzimidazolium dibromide salts, **1Br – 9Br** with Ag_2O in an equimolar ratio. After the separation by filtration from insoluble AgBr, the silver(I) di-NHC complexes were precipitated from methanolic solution by converting their respective silver(I) di-NHC dibromide into dihexafluorophosphate counterion through metathesis reaction as shown in **Scheme 2**. However, the obtained complexes of **Ag1 – Ag9** are lower in yield because during purification process, some of the complex is invariably lost. All the Ag(I) di-NHC complexes of **Ag7 – Ag15** were obtained in good yields. All the complexes are readily soluble in acetonitrile, DMSO, and insoluble in methanol, ethanol, diethyl ether and petroleum ether.
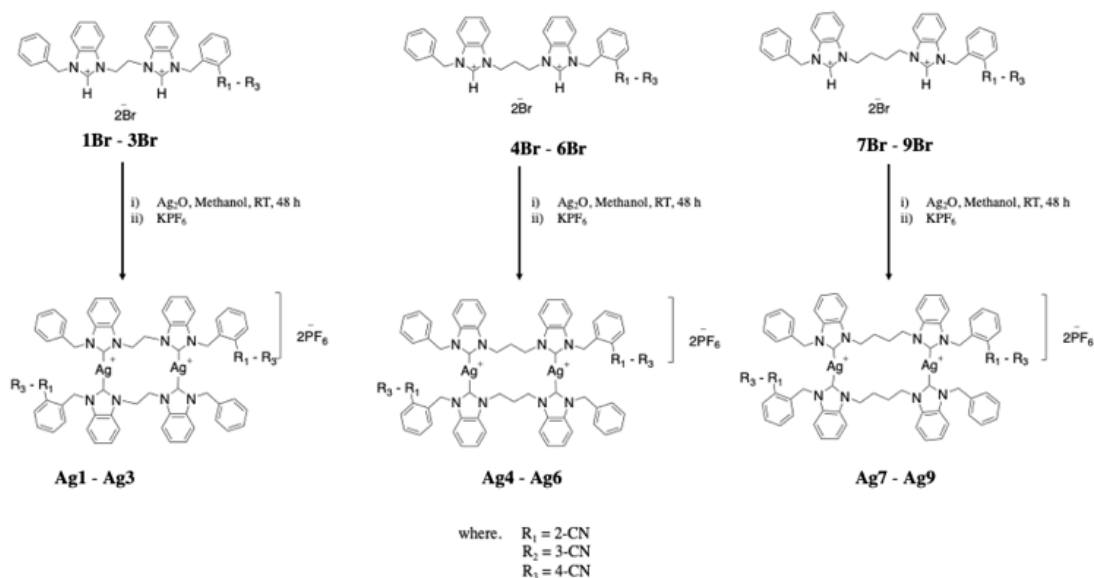
Scheme 2. The schematic diagram formation of nitrile functionalized silver(I) di-NHC complexes carrying different alkane bridges of ethylene/propylene/butylene.

The FTIR Analysis

The Fourier-transform infrared (FTIR) spectroscopy was employed to elucidate the structural characteristics and bonding nature of a series of novel nitrile-functionalized bis-benzimidazolium salts (**1Br** – **9Br**) and their corresponding dinuclear silver(I) di-NHC complexes (**Ag1** – **Ag9**). This spectroscopy analytical technique provided crucial insights into the molecular architecture and electronic properties of the synthesized compounds.

The FTIR spectra of the bis-benzimidazolium salts exhibited a distinctive sharp band in the range of 1558 – 1569 cm^{-1}, attributed to the ν(C=N) vibrations of the imidazolium moiety. Compound **7Br** as shown in **Figure 1** served as a representative example, showcasing this characteristic spectral feature. Upon complexation with Ag$^+$ ions, a significant bathochromic shift of this band to 1442 – 1459 cm^{-1} was observed across all complexes. This shift is indicative of the formation of a ν(C-N) module within the benzimidazole ring, providing strong evidence for the successful coordination of the NHC ligands to the silver centers [17]. Further spectral analysis revealed additional characteristic bands that corroborated the proposed structures of ν(Csp^2-H$_{aromatic}$) stretching observed in the range of 3028 – 3103 cm^{-1}, confirming the presence of aromatic moieties. Next, the ν(Csp^3-H$_{aliphatic}$) stretching was detected between 2926 – 2967 cm^{-1}, indicating the aliphatic linkers between the benzimidazole

units. A sharp band in the range of 2227 – 2239 cm⁻¹ was observed for the ν(C≡N) stretching validating the presence and retention of the nitrile functionality throughout the synthesis process.

Notably, the silver(I) complexes (**Ag1** – **Ag9**) exhibited absorption bands similar to their precursor salts, albeit with slight hypsochromic shifts and diminished intensities. This spectral behavior is consistent with the incorporation of silver centers into the molecular framework. The observed decrease in absorption intensity can be attributed to the electron-withdrawing effect of the coordinated silver ions, which modulates the electronic distribution within the ligand structure [17,18]. The retention of the ν(C≡N) stretching band in both the salts and complexes confirms the stability of the nitrile functionality during the complexation process. This observation is particularly significant, as it demonstrates the compatibility of the nitrile group with the silver-NHC coordination environment, potentially enabling further functionalization or catalytic applications. Moreover, the distinct shifts in the ν(C=N) and ν(C-N) bands provide compelling spectroscopic evidence for the successful formation of Ag-NHC bonds. These spectral changes align with previously reported silver(I)-NHC complexes in the literature, further corroborating the proposed structures of the synthesized dinuclear silver(I) di-NHC complexes.
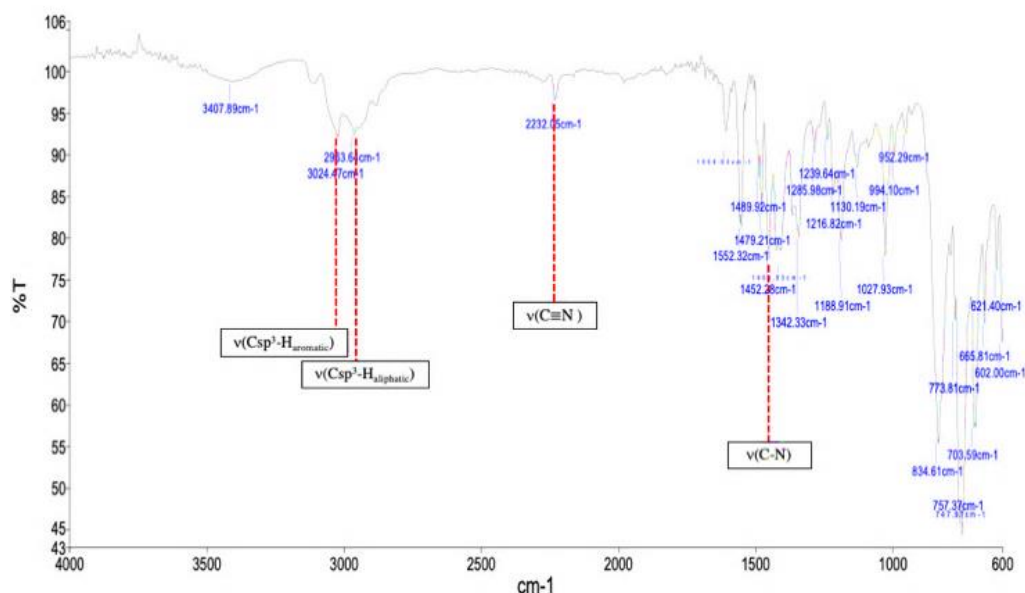
Figure 1. The FTIR spectra of **7Br** as representative for similar nitrile-functionalized bis-benzimidazolium salts in the same series.
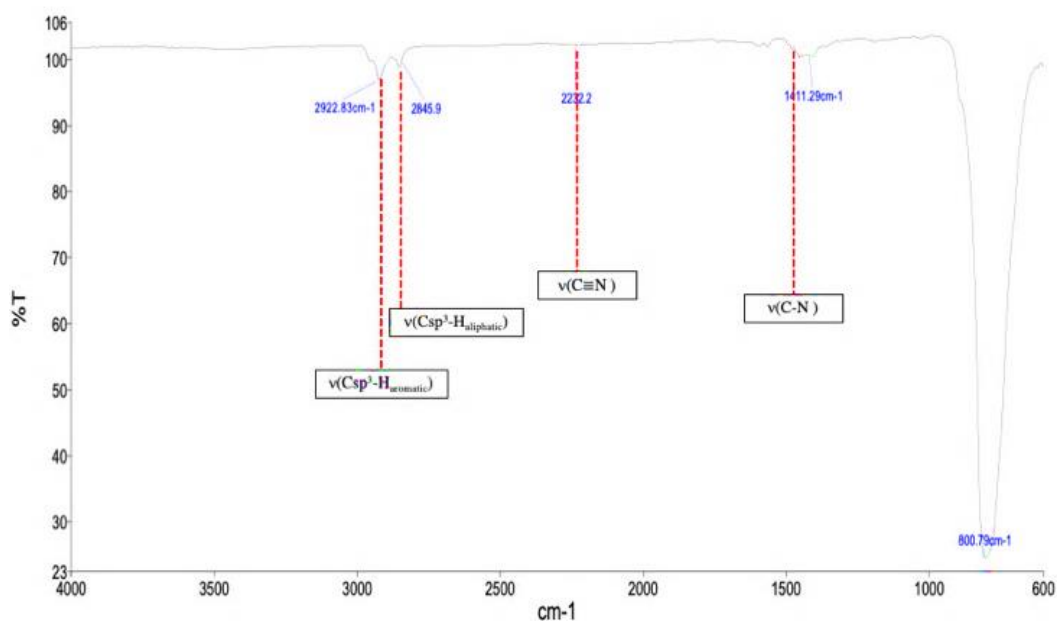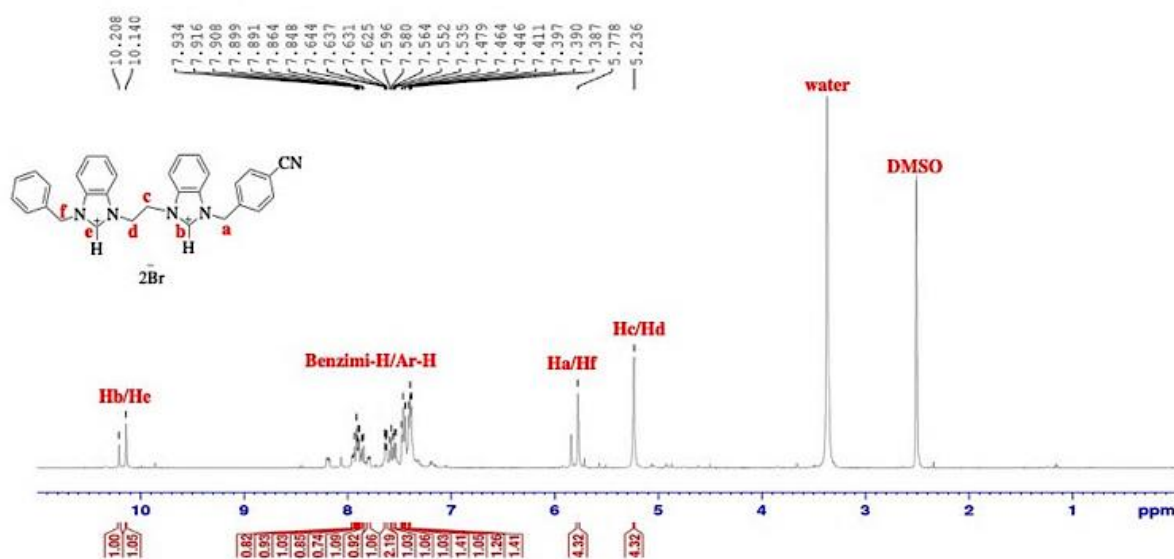
Figure 2. The FTIR spectra of **Ag7** as representative for similar nitrile-functionalized bis-benzimidazolium salts in the same series.

The ^{1}H- and ^{13}C-NMR Spectroscopy Analysis

The NMR spectra of all the nitrile-functionalized bis-benzimidazolium salts, **1Br** – **9PF$_6$** and their respective dinuclear Ag(I) di-NHC complexes, **Ag1** – **Ag9** were obtained in DMSO-d_6 over the scan range of δ 0 – 11 and δ 0 – 200 ppm for ^{1}H- and ^{13}C-NMR, respectively. In the upfield region appeared the resonances of the benzylic protons, -C<u>H</u>$_2$- for both benzyl and benzonitrile occurs between δ 5.74 – 6.03 ppm followed by different alkane chain terminal such as 1,2-ethanediyl, 1,3-propanediyl, and 1,4-butanediyl bridges at δ 5.20 – 5.28 (N-C<u>H</u>$_2$C<u>H</u>$_2$-N), δ 4.72 (N-CH$_2$C<u>H</u>$_2$CH$_2$-N), δ 5.72 (N-C<u>H</u>$_2$CH$_2$C<u>H</u>$_2$-N), δ 4.56 – 4.59 (N-CH$_2$C<u>H</u>$_2$C<u>H</u>$_2$CH$_2$-N) and δ 4.68 – 5.77 (N-C<u>H</u>$_2$CH$_2$CH$_2$C<u>H</u>$_2$-N), respectively. Nevertheless, the presence of two singlets at the range of δ 9.69 – 10.23 ppm, which corresponding to NC<u>H</u>N, indicate that the nitrile-functionalized bis-benzimidazolium salts were successfully formed.

After the conversion from bis-benzimidazolium salts, **1Br** – **9Br** towards the respective silver(I) di-NHC complexes, **Ag1** -**Ag9**, these acidic protons are removed by which, in all the ^{1}H-NMR spectra of Ag(I) di-NHC complexes, no signal was observed in the downfield region around δ 10 – 11 ppm, suggesting the complexion between the bis-benzimidazolium salts and Ag$^+$ ions (*vide infra*) was successful [19]. This observation is consistent with the deprotonation

of the benzimidazolium moieties and subsequent coordination to silver centres. The chemical shifts of other protons are similar to those reported before [20].

In the ^{13}C NMR spectra, the bis-benzimidazolium salts apart from the chemical shifts peaks of benzylic, alkane chain terminal, cyano group and aromatic carbons, the most characteristic resonances are two carbon peaks arises at around δ 142.84 – 143.70 and 143.05 – 143.09 ppm, respectively. This resonance due to the most deshielded of the two C2 carbons present in different chemical environment of the bis-benzimidazolium salts. All other carbon peaks are consistent with the chemical shifts as reported before [21]. Upon deprotonation and coordinating to the Ag$^+$ ions, the C2 carbons (C$_{carbene}$-Ag) are further deshielded, resulting in the shifts of the chemical shift to approximately δ 170.89 – 195.90 ppm. This variability may be attributed to factors such as the differing alkyl linker lengths, potential argentophilic interactions, or subtle differences in the coordination geometry around the silver centres. Further investigation of this phenomenon could provide valuable insights into the structure-property relationships of these novel complexes.

Figure 3. The ^{1}H-NMR spectra (d_6-DMSO, 500 MHz) of **9Br** as representative for similar nitrile-functionalized bis-benzimidazolium salts in the same series.
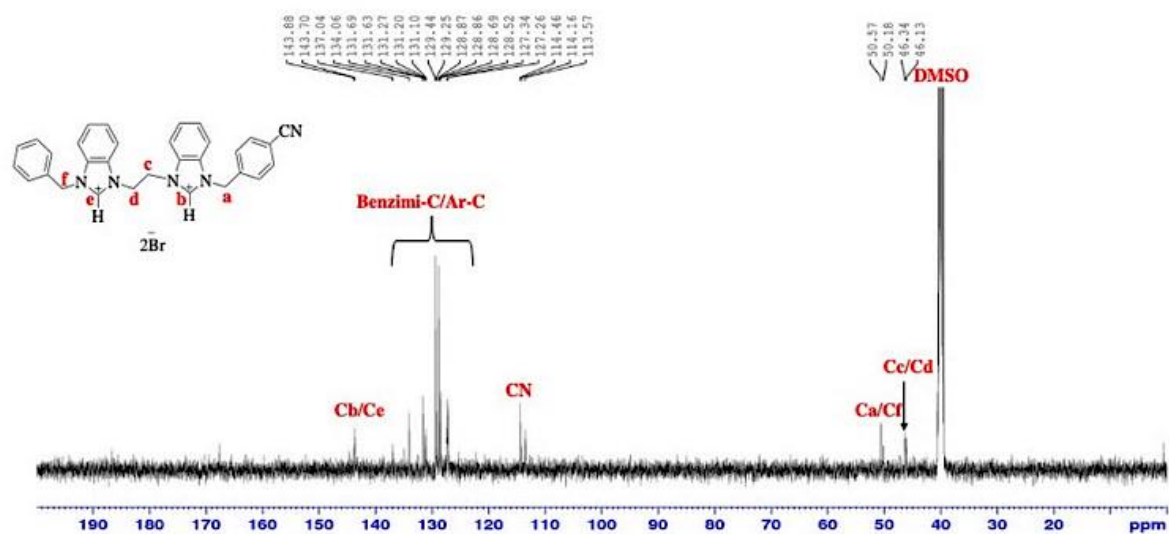
Figure 4. The ^{13}C-NMR spectra (*d₆*-DMSO, 125 MHz) of **9Br** as representative for similar nitrile-functionalized bis-benzimidazolium salts in the same series.
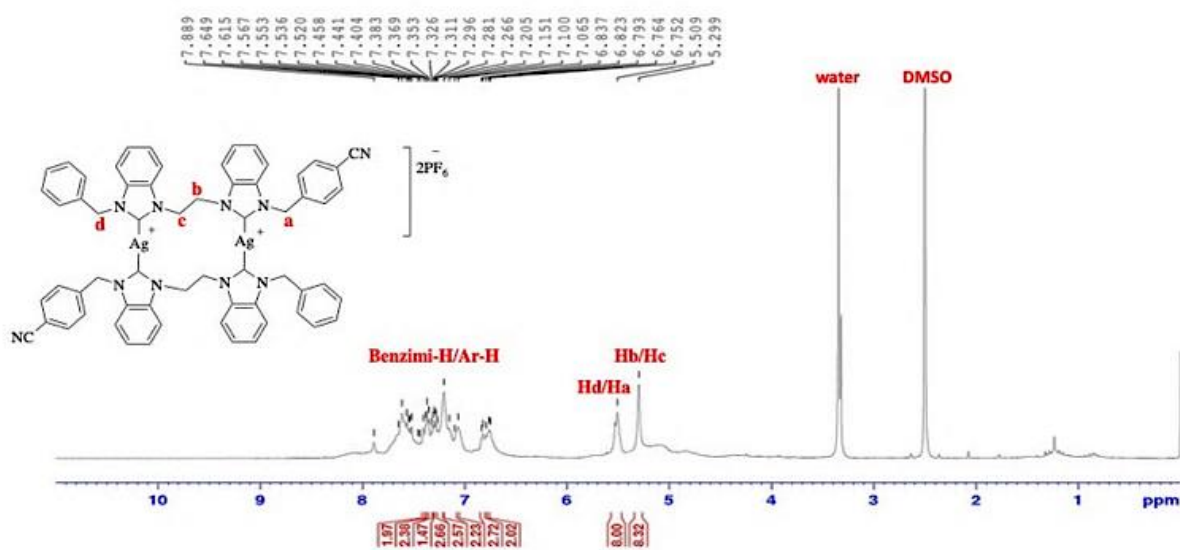

Figure 5. The ^{1}H-NMR spectra (*d₆*-DMSO, 500 MHz) of **Ag9** as representative for similar nitrile-functionalized dinuclear Ag(I) di-NHC complexes in the same series.
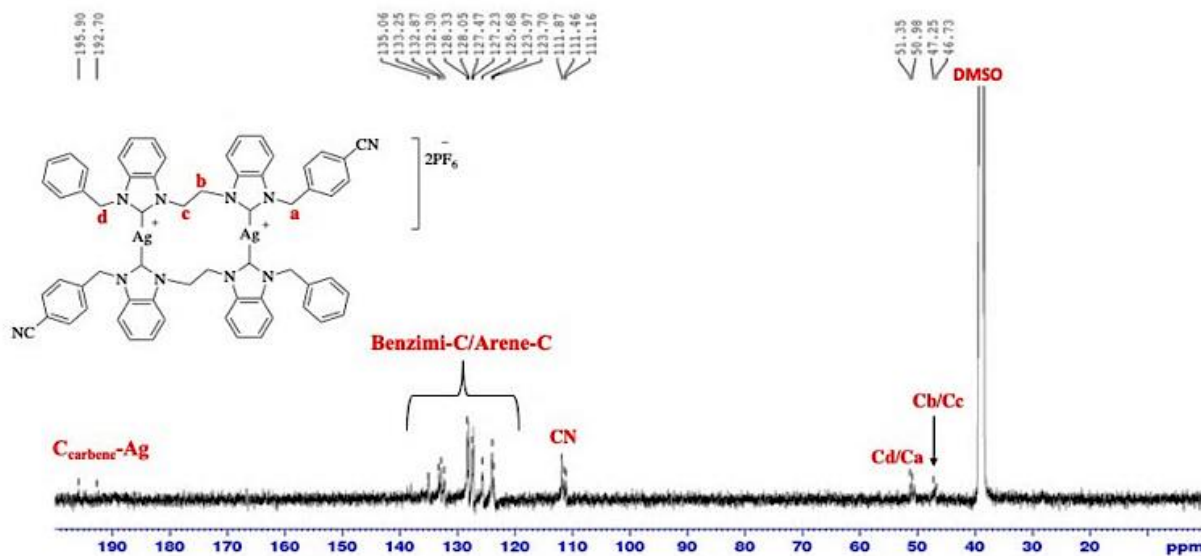
Figure 6. The ^{13}C-NMR spectra (d_6-DMSO, 125 MHz) of **Ag9** as representative for similar nitrile-functionalized dinuclear Ag(I) di-NHC complexes in the same series.

The Principal Component Analysis (PCA)

The chemometric of principal component analysis (PCA) were then employed to identify the correlations and relationships among the nitrile-functionalized bis-benzimidazolium salts and their respectives silver(I) di-NHC complexes based on their ^{1}H- and ^{13}C-NMR spectroscopic data. It is noted that the PCA is the powerful chemometric technique that reduces the dimensionality of sofiscated datasets while retaining most of the relevant information. It achieves this aforementioned advantage through transforming the original variables into new orthogonal variables known as principal components (PC) which are linear combinations of the original variable.
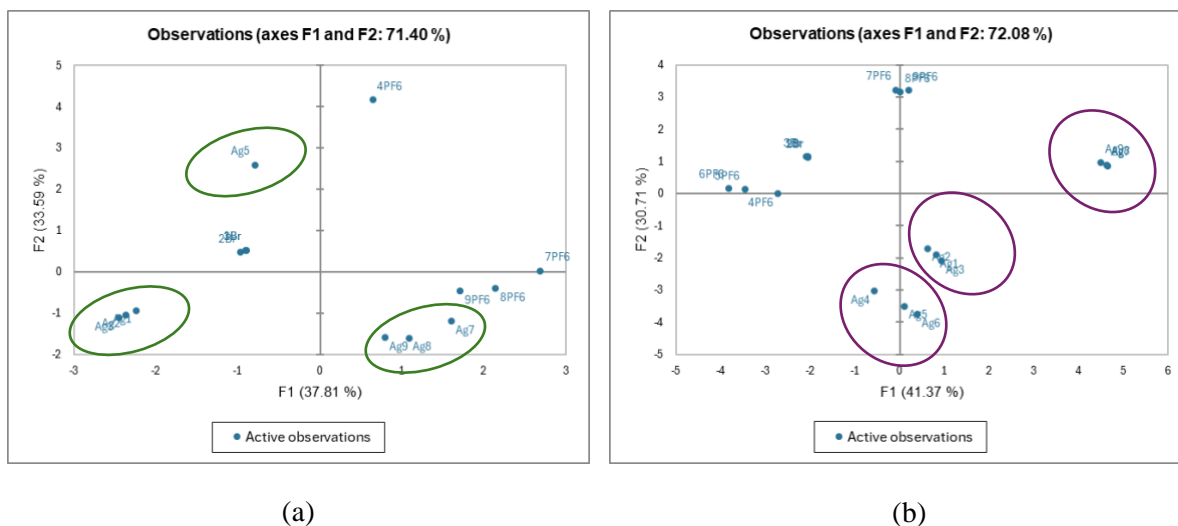
Figure 7. The principal component analysis (PCA) of (a) ^{1}H-NMR nitrile-functionalized bis-benzimidazolium salts with respective silver(I) di-NHC complexes with the observation/variables value of 71.40%; and (b) 13C-NMR nitrile nitrile-functionalized bis-benzimidazolium salts with respective silver(I) di-NHC complexes with the observation/variables value of 72.08%

In this study, the ^{1}H- and ^{13}C-NMR data were pre-processed by converting the NMR spectral data to an appropriate format of .xlsx and it then were imported into the XLSTAT software. The KMO test was performed to assess the adequacy of the dataset for the PCA with its value above 0.5 to be considered as acceptable [22]. The obtained KMO scores for this study were 0.678 and 0.760 for the ^{1}H and ^{13}C-NMR spectral data, indicated that the datasets were suitable for the PCA analysis.

Subsequently, the PCA was performed based on the NMR spectral data to maximize the variance among all the bis-benzimidazolium salts and its respective silver(I) di-NHC complexes, thus enhancing the ability to discern patterns and relationships. Noteworthy, the PCA is a widely used technique in chemometrics for dimensionality reduction and data visualization, which aids in identifying the most significant variations within the complex datasets [22]. The number of principal components (PCs) retained was optimized to obtain the best differentiation among the samples, as visualized through score plots as this process involved selecting the optimal number of PCs that explain the maximum variance while minimizing noise, as demonstrated by previous studies [23].

Meanwhile, the quality of the PCA models was evaluated using the R^2 and Q^2 values, which represent the goodness of fit and predictive ability, respectively. The R^2 value indicates the proportion of variance in the data explained by the model, while the Q^2 value reflects the model's ability to predict unseen data [23]. These metrics provide a robust assessment of the PCA model's reliability, ensuring that it can generalize well to new datasets.

The PCA score plot for the ^{1}H-NMR data in Figure 7 showed a clear separation and clustering of the benzimidazolium salts and their corresponding silver(I)-NHC complexes along the first two principal components (PCs), which captured 37.81% and 33.59% of the total variance, respectively. The cumulative observation value of 71.40% indicated that the PCA model could explain most of the variation in the ^{1}H-NMR data. Similarly, the PCA score plot for the 13C-NMR data (Figure 7) revealed a distinct clustering of the benzimidazolium salts, silver(I)-NHC complexes, and palladium(II)-NHC complexes based on their structural similarities and differences. The first two PCs accounted for 41.37% and 30.71% of the total variance, respectively, with an overall observation value of 72.08%,suggesting that the PCA model could capture a significant portion of the variance in the ^{13}C NMR data. It can be concluded that the PCA analysis was useful for correlating and classifying the benzimidazolium salts and their corresponding NHC complexes based on the NMR spectroscopic data.

The clear differentiation observed in the score plots implies that the NMR data contained sufficient information to distinguish the compounds based on their structural features and the presence/absence of specific functional groups (e.g., nitrile). Such a high cumulative variance is indicative of a robust model, consistent with findings in the literature where PCA is applied to spectroscopic data to reveal subtle but significant differences between chemical [24,25]. The results underscore the utility of PCA in chemometrics, particularly in the analysis of complex NMR datasets, where it aids in uncovering meaningful patterns that might not be apparent through traditional analytical methods.

CONCLUSION

In conclusion, the asymmetrical nitrile-functionalized silver(I) di-NHC complex of **Ag1** – **Ag9** as well as the bis-benzimidazolium salt **1Br** – **9Br** were also successfully synthesized. The Ag(I) di-NHC complexes and generated bis-benzimidazolium salts were all studied using FTIR, ^{1}H- and ^{13}C-NMR spectroscopies, and CHN elemental analysis, among other

spectroscopic methods. Despite encountering challenges such as the application of the synthesized asymmetrical dinuclear Ag(I) di-NHC complexes, we remain optimistic about the potential implications of this research. Moving forward, it is crucial to address the remaining aspects of the synthesis works as anticancer, antimicrobial, catalysis studies and many more. Completing this work in the future has the potential to significantly advance the understanding of inorganic synthesis of silver(I)-NHC complexes and contribute to the chemistry field. We are excited about the prospects for future research in this research area and remain committed to furthering our efforts to overcome current challenges and achieve our objectives.

ACKNOWLEDGEMENT

AUTHORS CONTRIBUTIONS

M. Z. Nazri conceptualization, writing – original draft, investigations and formal analysis. **M. R. Razali** conceptualized the central research idea, validation, supervision and funding acquisition. **S. Y. Hussaini** and **N. Basar** anchored the review, validation, revisions and approved the articled submission.

CONFLICT OF INTEREST

The authors declare no conflict of interest.

REFERENCES

[1]   Jalal, M., Hammouti, B., Touzani, R., Aouniti, A., & Ozdemir, I. (2020). Metal-NHC Heterocycle Complexes in Catalysis and Biological Applications: Systematic Review. *Materials Today: Proceedings*, *31*, S122-S129. https://doi.org/10.1016/j.matpr.2020.06.398

[2]   Li, J., He, D., Lin, Z., Wu, W., & Jiang, H. (2021). Recent Advances in NHC–Palladium Catalysis for Alkyne Chemistry: Versatile Synthesis and Applications. *Organic Chemistry Frontiers*, *8*(13), 3502-3524. https://doi.org/10.1039/D1QO00111F

[3]   Wang, Z., Tzouras, N. V., Nolan, S. P., & Bi, X. (2021). Silver *N*-Heterocyclic Carbenes: Emerging Powerful Catalysts. *Trends in Chemistry*, *3*(8), 674-685. https://doi.org/10.1016/j.trechm.2021.04.006

[4]   Ronga, L., Varcamonti, M., & Tesauro, D. (2023). Structure–Activity Relationships in NHC–Silver Complexes as Antimicrobial Agents. *Molecules*, *28*(11), 4435. https://doi.org/10.3390/molecules28114435

[5]   Scattolin, T., & Nolan, S. P. (2020). Synthetic Routes to Late Transition Metal–NHC Complexes. *Trends in Chemistry*, *2*(8), 721-736. https://doi.org/10.1016/j.trechm.2020.06.001

[6]   Nayak, S., & Gaonkar, S. L. (2021). Coinage Metal *N*-Heterocyclic Carbene Complexes: Recent Synthetic Strategies and Medicinal Applications. *ChemMedChem*, *16*(9), 1360-1390. https://doi.org/10.1002/cmdc.202000836

[7]   Şahin-Bölükbaşı, S., & Şahin, N. (2019). Novel Silver-NHC Complexes: Synthesis and Anticancer Properties. *Journal of Organometallic Chemistry*, *891*, 78-84. https://doi.org/10.1016/j.jorganchem.2019.04.018

[8]   Romain, C., Bellemin-Laponnaz, S., & Dagorne, S. (2020). Recent Progress on NHC-Stabilized Early Transition Metal (Group 3–7) Complexes: Synthesis and Applications. *Coordination Chemistry Reviews*, *422*, 213411. https://doi.org/10.1016/j.ccr.2020.213411

[9]   Werner, L., Horrer, G., Philipp, M., Lubitz, K., Kuntze-Fechner, M. W., & Radius, U. (2021). A General Synthetic Route to NHC-Phosphinidenes: NHC-Mediated Dehydrogenation of Primary Phosphines. *Zeitschrift für anorganische und allgemeine Chemie*, *647*(8), 881-895. https://doi.org/10.1002/zaac.202000405

[10]   Aktaş, A., Yakalı, G., Demir, Y., Gülçin, İ., Aygün, M., & Gök, Y. (2022). The Palladium-Based Complexes bearing 1,3-dibenzylbenzimidazolium with Morpholine, Triphenylphosphine, and Pyridine Derivate Ligands: Synthesis, Characterization, Structure and Enzyme Inhibitions. *Heliyon*, *8*(9). https://doi.org/10.1016/j.heliyon.2022.e10625

[11]   Giarrusso, C. P., Zeil, D. V., & Blair, V. L. (2023). Catalytic exploration of NHC–Ag (i) HMDS Complexes for the Hydroboration and Hydrosilylation of Carbonyl

Compounds. *Dalton Transactions*, *52*(23), 7828-7835. https://doi.org/10.1039/D3DT01042B

[12]   Abdurrahman, N., Sasidharan, S., Mudzakir, A., Yoshinari, N., & Razali, M. R. (2023). A Symmetrical Tetra *N*-Heterocyclic Carbene Binuclear Silver(I) Complex: Synthesis, Characterization and Anticancer Study. *Journal of Coordination Chemistry*, *76*(16-24), 1921-1940. https://doi.org/10.1080/00958972.2023.2289001

[13]   Fatima, T., Haque, R. A., Ahmad, A., Hassan, L. E. A., Ahamed, M. B. K., Majid, A. A., & Razali, M. R. (2020). Tri N-Heterocyclic Carbene Trinuclear Silver(I) Complexes: Synthesis and In-vitro Cytotoxicity Studies. *Journal of Molecular Structure*, *1222*, 128890. https://doi.org/10.1016/j.molstruc.2020.128890

[14]   Lumivero (2024). XLSTAT Statistical and Data Analysis Solution. https://www.xlstat.com/en.

[15]   Nazri, M. Z., Zaini, N. S. M., Kamaruddin, N. N., Rameezal, R. N., Musa, N. F., Razali, M. R. & Basar, N. (2024). Synthesis, Characterizations and Multivariate Data Analysis of Non- and Nitrile-Functionalized Silver(I) and Palladium(II) *N*-Heterocyclic Carbene Complexes. *Scientific Research Journal*, *21*(2), 89-117. https://doi.org/10.24191/srj.v21i2.26553

[16]   Sani, M. S. A., Ismail, A. M., Azid, A., Samsudin, M. S., & Yuswan, M. H. (2024). Incorporation of Partial Least Squares-Discriminant Analysis with Ultra-High-Performance Liquid Chromatography Diode-Array Detector for Authentication of Skin Gelatine Sources. *Halalsphere*, *4*(1), 1-13. https://doi.org/10.31436/hs.v4i1.83

[17]   Nazri, M. Z., Cilwyn, B., Huda, K., Sreenivasan, S., & Razali, M. R. (2023). Synthesis, Structural and Anticancer Studies of Asymmetrical Dinuclear Silver (I) Di-*N*-heterocyclic Carbene Complexes. *Malaysian Journal of Chemistry*, *25*(4), 207-221. https://doi.org/10.55373/mjchem.v25i4.207

[18]   Hussaini, S. Y., Haque, R. A., Haziz, U. F., Amirul, A. A., & Razali, M. R. (2021). Dinuclear Silver(I)- and Gold(I)-*N*-Heterocyclic Carbene Complexes of *N*-alkyl Substituted Bis-Benzimidazol-2-ylidenes with Aliphatic Spacer: Synthesis, Characterizations and Antibacterial Studies. *Journal of Molecular Structure*, *1246*, 131187. https://doi.org/10.1016/j.molstruc.2021.131187

[19]   Nadeem, R. Y., Yaqoob, M., Yam, W., Haque, R. A., & Iqbal, M. A. (2022). Synthesis, characterization and biological evaluation of Bis-benzimidazolium salts and their silver(I)-*N*-heterocyclic carbene complexes. *Medicinal Chemistry Research*, *31*(10), 1783-1791. https://doi.org/10.1007/s00044-022-02942-7

[20] Hussaini, S. Y., Haque, R. A., Li, J. H., Zhan, S. Z., Tan, K. W., & Razali, M. R. (2019). Coinage Metal Complexes of *N*-Heterocyclic Carbene Bearing Nitrile Functionalization: Synthesis and Photophysical Properties. *Applied Organometallic Chemistry*, *33*(6), e4927. https://doi.org/10.1002/aoc.4927

[21] Yeap, C. W., Haque, R. A., Yam, W. S., & Razali, M. R. (2019). The first Mesomorphic Benzimidazolium-based Silver(I)-*N*-Heterocyclic Dicarbene Complexes: Synthesis, Characterization and Phase Properties. *Journal of Molecular Liquids*, *277*, 341-348. https://doi.org/10.1016/j.molliq.2018.12.075

[22] Altuntaş, Ü., Güzel, İ., & Özçelik, B. (2023). Phenolic Constituents, Antioxidant and Antimicrobial Activity and Clustering Analysis of Propolis Samples based on PCA from Different Regions of Anatolia. *Molecules*, *28*(3), 1121. https://doi.org/10.3390/molecules28031121

[23] Jolliffe, I. T., & Cadima, J. (2016). Principal Component Analysis: A Review and Recent Developments. *Philosophical Transactions of the Royal Society A: Mathematical, Physical and Engineering Sciences*, *374*(2065), 20150202. https://doi.org/10.1098/rsta.2015.0202

[24] Bro, R., & Smilde, A. K. (2014). Principal component analysis. *Analytical methods*, *6*(9), 2812-2831. https://doi.org/10.1039/C3AY41907J

[25] Ibrahim, R. M., Eltanany, B. M., Pont, L., Benavente, F., ElBanna, S. A., & Otify, A. M. (2023). Unveiling the Functional Components and Antivirulence Activity of Mustard Leaves using an LC-MS/MS, Molecular Networking, and Multivariate Data Analysis Integrated Approach. *Food Research International*, *168*, 112742. https://doi.org/10.1016/j.foodres.2023.112742